Effect of Protic Ionic Liquid Nanostructure on Phospholipid Vesicle Formation

Saffron J. Bryant,[1] Kathleen Wood,[2] Rob Atkin[3] and Gregory G. Warr[1*]

1. School of Chemistry, F11, The University of Sydney, NSW 2006, Australia

2. Bragg Institute, ANSTO, Locked Bag 2001, Kirrawee DC, NSW 2232, Australia

3. Discipline of Chemistry, The University of Newcastle, Newcastle, NSW, Australia, 2308, Australia

ABSTRACT

The formation of bilayer-based lyotropic liquid crystals and vesicle dispersions by phospholipids in a range of protic ionic liquids has been investigated by polarizing optical microscopy using isothermal penetration scans, differential scanning calorimetry, and small angle X-ray and neutron scattering. The stability and structure of both lamellar phases and vesicle dispersions is found to depend primarily on the underlying amphiphilic nanostructure of the ionic liquid itself. This finding has significant implications for the use of ionic liquids in soft and biological materials and for biopreservation, and demonstrates how vesicle structure and properties can be controlled through selection of cation and anion. For a given ionic liquid, systematic trends in bilayer thickness, chain-melting temperature and enthalpy increase with phospholipid acyl chain length, paralleling behaviour in aqueous systems.

* Corresponding Author: Tel.: +61 2 9351 2106. E-mail: gregory.warr@sydney.edu.au

Introduction

Ionic liquids (ILs) are salts that melt below 100°C, with many forming liquids at or below room temperature. They are of great interest as potential replacements for organic solvents in a range of chemical processes, due to their low vapour pressures,[1, 2] as well as their ability to dissolve a wide variety and combination of solutes. Strikingly, many ILs have been shown to exhibit a solvophobic effect (analogous to the hydrophobic effect in water) by supporting surfactant aggregation into micelles, lyotropic liquid crystals and microemulsions,[3-5] and by stabilizing protein folding[6] and maintaining enzyme structure and activity for biocatalysis.[7] Understanding the factors that control structure in such soft and biological materials is critical to realizing diverse applications of ILs from their use as biopreservatives to the development of designer nanoreactors.[8, 9]

Protic ILs (PILs) in particular have been studied in this regard,[10] precipitated by studies showing that the archetype ethylammonium nitrate (EAN) can form a dense, three-dimensional H-bond network.[11] Being both cheaper and more easily synthesised than their aprotic analogues, they have greater potential for use at scale. Many PILs are also distillable due to proton exchange between cation or anion and their conjugate base or acid, facilitating recycling.

Like synthetic surfactants, phospholipids such as 1,2-dipalmitoyl-sn-glycero-3-phosphatidylcholine (DPPC) self-assemble in water and some other polar solvents due to solvophobic interactions between the solvent and the hydrocarbon chains.[8, 12-14] The two acyl tails of lipids favour planar packing geometries, which predisposes them to form lamellar phases, and leads to biphasic vesicle dispersions upon dilution.[12, 15-18] Vesicles are formed when a bilayer membrane encapsulates solvent, thus separating it from the external environment.[19]

Phospholipids are a major component of the membranes of living cells, which makes vesicles excellent models for examining prebiotic compartmentalization.[20] Lipid bilayer integrity is key to maintaining

cell function, so understanding how ILs affect bilayer stability will determine their viability as bio-preservatives, and also inform how biological processes may operate in extreme, even non-aqueous, environments.

Most previous studies of self-assembly in ionic liquids have focused on micelle formation by conventional, water-soluble synthetic surfactants.[21-25] Few have examined self-assembly of water-insoluble amphiphiles such as didodecyldimethylammonium bromide in ethylammonium nitrate (EAN)[23] or lipids like DPPC in various aprotic ILs.[8]

Unlike water, many ILs are themselves amphiphilically nanostructured.[26] This nanostructure arises from the strong coulomb forces between charged centres which, together with an H-bond network, leads to charged domains that solvophobically expel non-polar moieties (typically cation alkyl chains) into segregated domains. The extent and nature of this nanostructure depends on cation and anion type, and can strongly impact the solubility of various solutes. This is clearly seen, for example, in surfactant critical micelle concentrations, which are much higher in nanostructured ILs than in water. Similarly, longer alkyl chains are found necessary for lyotropic phase formation by surfactants in nanostructured ILs than in water.[4, 27]

Here we investigate the equilibrium phase behavior and vesicle formation by phospholipids of varying alkyl tail lengths in a selected set of protic ILs in order to understand how changes in ion structure and hence IL nanostructure influences lamellar phase and vesicle formation, structure and stability.

Figure 1 shows the structure of the PILs examined. Of the primary ammonium salts, propylammonium nitrate (PAN) exhibits the strongest amphiphilic nanostructure,[28] consisting of interpenetrating bicontinuous networks of polar and nonpolar domains, with polar domains consisting of ammonium and nitrate charge centres associated in an extended, three-dimensional H-bond network. This bicontinuous structure is still present but less pronounced in ethylammonium nitrate (EAN), and is further diminished

when nitrate is replaced with formate (EAF). Ethanolammonium formate (EtAF) is only weakly nanostructured, as polar-apolar sequestration is interrupted by the terminal hydroxyl group participating in the H-bond network.[29, 30] The liquid structure of dimethylethylammonium formate (DMEAF) has been less well-studied: DMEAF cannot form an extended H-bond network, so the driving force for its liquid nanostructure is entirely electrostatic. Indirect evidence comparing IL interfacial structure suggests that DMEAF will also only be weakly structured in bulk.[31, 32]

The phase behavior of various phospholipids in these PILS was characterized by isothermal penetration scans[33] using polarizing optical microscopy complemented by small-angle X-ray scattering. This was contrasted with vesicles prepared by the ethanol injection method,[34] with their structure and properties determined using a combination of polarizing microscopy, differential scanning calorimetry (DSC) and small-angle neutron scattering (SANS).

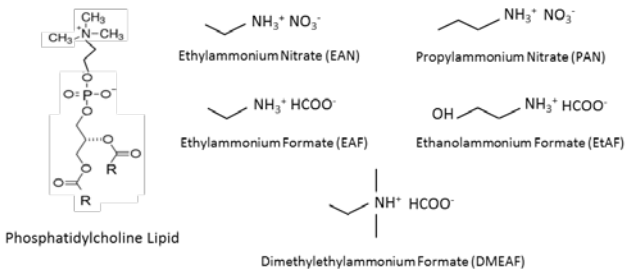

Figure 1. Structures of the ILs and lipids used in this work, where R = $C_{13}H_{27}$ (DMPC); $C_{15}H_{31}$ (DPPC); $C_{17}H_{35}$ (DSPC); or a mixture (egg PC).

Materials and Methods

Ionic liquids were prepared by reacting equimolar amounts of nitric (Ajax Finechem, 70%) or formic (Sigma-Aldrich, 98%) acid with the bases ethylamine (Sigma-Aldrich, 70%), ethanolamine (Merck, 98%), propylamine (Sigma-Aldrich, 70%) or dimethylethylamine (Sigma-Aldrich, 99%) to produce aqueous solutions of ionic liquids as previously described.[25] Excess water was removed by rotary evaporation followed by freeze-drying. Additional drying with phosphorous pentoxide was used as required. Using this method the following protic ionic liquids were generated; ethylammonium nitrate (EAN), propylammonium nitrate (PAN), ethylammonium formate (EAF), ethanolammonium formate (EtAF), and dimethylethylammonium formate (DMEAF) (see Figure 1).

Deuterated ionic liquids for SANS were made by repeated exchange with D_2O in order to deuterate the ammonium ions.

Karl Fischer titration was used to ensure water removal to below 0.01 %w/w and nuclear magnetic resonance was used to confirm correct ionic liquid formation for both hydrogenous and deuterated products.

Four different phosphatidylcholine (PC) lipids were used as shown in Figure 1. Three contained saturated alkyl chains of differing lengths; 1,2-dimyristoyl-sn-glycero-3-phosphocholine (DMPC), 1,2-dipalmitoyl-sn-glycero-3-phosphocholine (DPPC), 1,2-distearoyl-sn-glycero-3-phosphocholine (DSPC), while the fourth, egg PC, is a mixture containing 1-palmitoyl-2-oleoyl-sn-glycero-3-phosphocholine (POPC) as its majority constituent. All lipids were purchased from Sigma-Aldrich with ≥99% purity and used as received.

Isothermal penetration experiments were performed as previously described[4, 33] to examine lyotropic phase formation over a range of concentrations. Briefly, a small amount of lipid, approximately 40μm thick, was placed between a microscope slide and a coverslip. A drop of IL was placed on the outer edge

of the coverslip and was drawn in by capillary action. This creates a concentration gradient from pure IL to pure lipid. Polarising optical microscopy was used to identify phases across the concentration gradient based on optical signatures.[35] The microscope stage was heated from room temperature to 353 K to examine phase changes with temperature.

Selected samples at fixed compositions were also examined by SAXS using an Anton Paar SAXSess and 1mm path length quartz capillary cells. The samples consisted of 12wt% DMPC or 18wt% DPPC in EAN, both of which were analysed at a range of temperatures, and scattering collected for 10mins.

Dilute vesicle dispersions were generated using the ethanol injection method.[34] The lipids were dissolved in ethanol and then injected into the relevant solvent. Ethanol was removed using rotary evaporation. The final concentration of lipid after ethanol evaporation was 1 wt% for DSC and 0.6 wt% for SANS. Dynamic light scattering (Malvern Zetasizer Nano ZS) was routinely used as a preliminary confirmation of the presence of dispersed particles, yielding diameters consistent with the SANS results.

Differential scanning calorimetry of lipid dispersions was carried out on a Mettler Toledo DSC823 using standard procedures. Samples prepared using the ethanol injection method to a final concentration of 1 wt% lipid, were placed into sealed aluminium pans and heated at 5°C /min under nitrogen to a maximum of 70°C. All heating ranges included the chain melting temperature of the respective lipid.

Small-angle neutron scattering was performed on 0.6 wt% phospholipid dispersions at temperatures from 25°C to 65°C as previously described on the QUOKKA[36] beamline at ANSTO.[21] Detector distances of 1.35m (with 20cm detector offset), 8m and 20m (with and without lenses) were used with 5 Å neutrons (8.1 Å with lenses) for a combined q range of 0.001-0.7Å^{-1}. Data reduction was performed with Igor Pro using the modified reduction macros from the NCNR.[37] SANS data was analysed using SASview to determine the best fit parameters to a range of candidate structural models for each data set.

Results

Isothermal Penetration Studies. All phospholipid mixtures in all ILs examined exhibited the characteristic optical texture of a lyotropic lamellar phase under crossed polarisers,[33, 38] except for DMPC and DPPC in EAN and PAN.

At (and even below) room temperature, egg PC formed myelinic figures over time, indicating a swollen and dispersible (L_α) lamellar phase. Maltese cross textures subsequently appeared, which are diagnostic for vesicle formation.[38-41] While egg PC spontaneously generated vesicles at room temperature in water and in all of the ionic liquids, the saturated-chain phospholipids (DPPC, DMPC and DSPC) only formed vesicles above a minimum swelling temperature (T_s), as shown in Table 1. Figure 2 shows representative polarising optical micrographs of the optical textures of a non-swelling lamellar phase of DMPC in EtAF at 30 °C, and the formation of myelinic figures and vesicles at 36 °C. In water, the measured T_s was consistent with previous reports,[15] and showed a clear increase with alkyl chain length. The same pattern was observed for phospholipids in the formate ILs and for DSPC in EAN and PAN, but in each case T_s was several degrees higher than in water. Neither DMPC nor DPPC formed obvious swellable lamellar phases in EAN or PAN. DPPC instead formed a hexagonal phase in both ILs whilst the DMPC phase could not be identified. The temperatures of these transitions, to either a hexagonal phase in the case of DPPC or to an unidentified phase in the case of DMPC, are also listed in Table 1. DSPC in EAN and PAN formed vesicles at temperatures higher than the other solvents.

Table 1. Minimum swelling temperatures (T_s) for lamellar phases compared with lipid chain melting temperatures (T_m) and associated chain melting enthalpy and entropy for 1 wt% DMPC, DPPC and DSPC vesicles in water and several protic ionic liquids. Square brackets indicate an observed transition that was not lamellar.

		T_s (K)	T_m (K)	$\Delta H°_t$ (kJ mol^{-1})	$\Delta S°_t$ (J mol^{-1} K^{-1})
DMPC	H_2O	296 (296)[15]	297.5 (294)[42]	13.5 (15)[42]	45 (52.3)[42]
	EAN	[322]	-	-	-
	PAN	[318]	-	-	-
	EAF	303	299	8	20
	EtAF	309	296	12	40
	DMEAF	296	296	9	31
DPPC	H_2O	314 (314)[15]	314 (310.5)[42]	26 (25)[42]	85 (82)[42]
	EAN	[323]	316	14	45
	PAN	[323]	312	19	60
	EAF	323	317	21	65
	EtAF	324	313	29	93
	DMEAF	314	313	26	84
DSPC	H_2O	329 (327)[15]	328 (324)[42]	38 (37)[42]	114 (115)[42]
	EAN	339	329 (330)[43]	23	69
	PAN	339	325	23	69
	EAF	333	-	-	-
	EtAF	337	-	-	-
	DMEAF	324	-	-	-

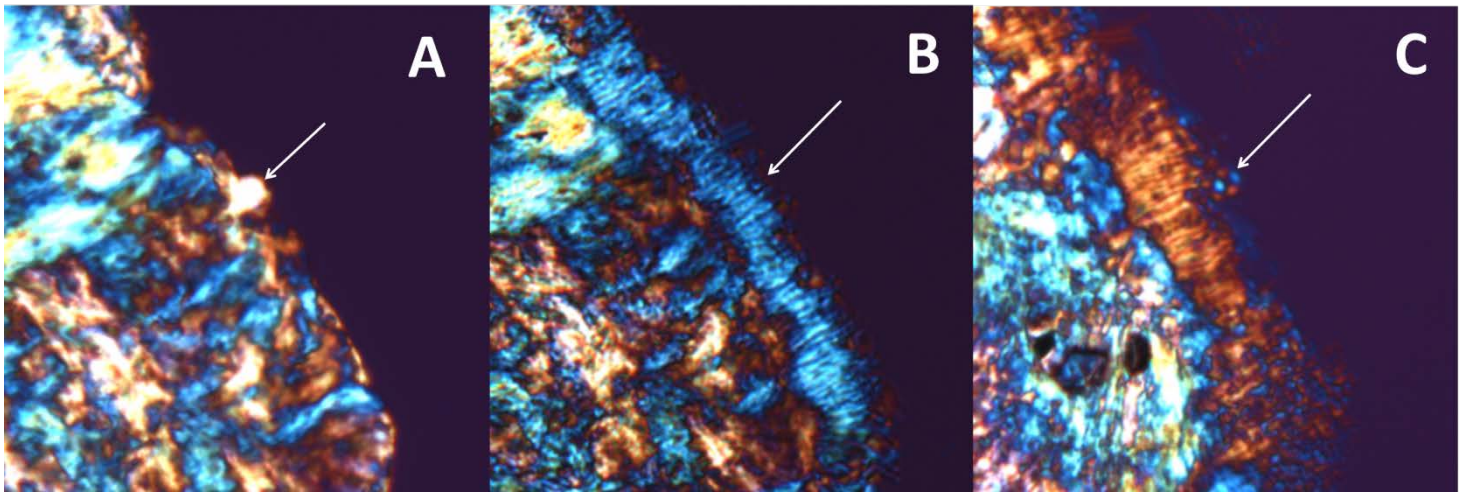

Figure 2. Polarising optical micrographs of DMPC in EtAF isothermal penetration scan showing (A) lamellar texture at 30°C; (B) myelinic figures growing into the ionic liquid at 36°C, and (C) subsequent appearance of Maltese cross textures (vesicles) at 36°C.

Vesicle Dispersions. The properties of the phospholipid assemblies formed by isothermal swelling were compared with vesicle dispersions prepared by ethanol injection and evaporation. Differential scanning calorimetry (DSC) was used to determine the chain melting temperature, T_m, of lipids in dilute (1 wt%) vesicle dispersions. These are listed in Table 1.

In water, T_m of saturated chain lipids agreed with previous reports, as did the corresponding chain melting enthalpies and entropies.[42] No transition temperature could be measured for egg PC, because it is a mixture of lipids.

As observed in water, the chain melting temperatures of saturated chain lipids in all ionic liquids measured were found to increase with alkyl tail length (see Table 1). We were unable to reliably measure T_m of DSPC in any of the formate ILs due to a broad endotherm observed at high temperatures, which ob-

scures any chain melting transition peak. This endotherm is attributed to evaporation of the formate ionic liquids.[44 45]

There was close agreement between T_m and T_s in water and DMEAF, but in EAF and EtAF T_s systematically exceeds T_m by a few degrees. This is probably a consequence of the high viscosity of these ILs slowing the swelling process during warming of the bulk microscopy samples. In EAN and PAN chain melting transition temperatures were observed for DPPC and DSPC but, as with the other ILs, were lower than T_s seen with microscopy, again suggesting a viscosity effect. Evans *et al*. reported a T_m of 330 K for DSPC in EAN, consistent with the results presented here.[43]

The chain melting enthalpies of DMPC and DPPC are comparable in EtAF and in water, but significantly smaller in EAF, EAN, and PAN. DPPC in DMEAF is also water-like in this respect. This suggests that the amphiphilic nanostructure of the IL plays a role in phospholipid vesicle stability.

Despite numerous scans, no T_m could be detected for DMPC in either nitrate IL. This is probably due to their transition enthalpies being too small to be detected, based on extrapolation of the values for DPPC and DSPC.

SANS measurements on 0.6 wt% phospholipid dispersions prepared by ethanol injection in water (D_2O) and various partially-deuterated ILs confirmed the presence of micron-sized aggregates. Figure 3 shows SANS patterns of egg PC dispersions, which form unilamellar vesicles (ULVs) in all solvents examined except PAN at 25 °C. As a general analysis protocol, each scattering pattern was analysed using a range of models of increasing complexity, beginning with homogeneous spheres,[46] multilamellar vesicles (MLV),[47] and unilamellar vesicles as both free bilayers[46] and using a separated form factor model,[48] which accounts for the effect of solvent penetration between polar groups and into the bilayer on the scattering length density.[48] Solvent penetration was modelled as both a constant and as a linear gradient in scattering length density. A full data set for all lipids in all solvents at all temperatures examined is

provided in the Supplementary Information, together with lines of best-fit and fitting parameters, and further discussion of the models used.

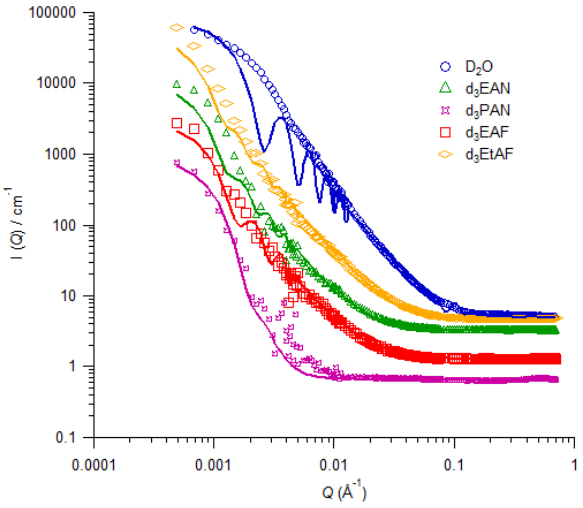

Figure 3. SANS patterns and model fits for 0.6wt% egg PC in D_2O and partially deuterated ILs at 298K, prepared by the ethanol injection method. Arbitrary offset on the y-axis for clarity. Solid lines show best fits (see text).

The best-fit structures for each lipid in the various solvents are summarised in Table 2. As expected, all lipids examined formed unilamellar vesicles in D_2O both above and below T_m. Best–fit values for the overall bilayer thicknesses of ULVs are listed in Table 3, The range shown reflects the different models for polar-group hydration chosen,[46, 48] but for water are in good agreement with previous SAXS and SANS studies.[17, 48-63]

Table 2. Summary aggregate morphologies – uni- or multi-lamellar vesicles, ULV and MLV, or homogeneous spheres - found by fitting SANS data for lipids in D_2O and ionic liquids above T_m. Morphology below T_m shown in parentheses if different.

	Egg PC	DMPC	DPPC	DSPC
D_2O	ULV	ULV	ULV	ULV
EAN	ULV	MLV	MLV	MLV
PAN	Sphere/MLV	Sphere	MLV	MLV
EAF	ULV	MLV	MLV	ULV (MLV)
EtAF	ULV	MLV	ULV (MLV)	ULV
DMEAF	-	-	ULV (MLV)	ULV (MLV)

The formation of ULVs by egg PC at 298K in all ILs examined except PAN, is consistent with our observations of isothermal penetration microscopy. SANS clearly shows (Figure 3) that egg PC assembled into similarly-sized aggregates in PAN as in the other solvents, but the scattering pattern could not be fit to unilamellar vesicles with physically plausible bilayer dimensions. Modeling as polydisperse, homogeneous spheres or as weakly ordered multilamellar vesicles yielded an adequate description of the SANS pattern, but we could not discriminate between the two structures. Optical microscopy of these systems suggests MLVs.

All saturated alkyl chain phospholipid dispersions behaved very differently in ILs than in water. All dispersions in all solvents were prepared below T_m at 296 K, but in ILs this resulted in SANS patterns consistent with the formation of multilamellar vesicles rather than ULVs, in every case except DSPC in

EtAN (see Supplementary Information Figures S2-S8). MLVs were easily identified as they exhibited a diffraction peak in the vicinity of q = 0.1 Å^{-1} (see inset to Figure 4), corresponding to the repeat spacing of the bilayers, or 'onions.' Upon heating above T_m, DSPC in EAF and DMEAF and DPPC in EtAF and DMEAF transformed into ULVs (Table 2) but MLVs were retained and the scattering spectra were virtually unchanged in all other systems. While the position of the diffraction peak was reproducible, its intensity and sharpness depended on sample history, especially heating and cooling. This indicates that the number and order of bilayer stacking is not necessarily equilibrated in these systems. This is consistent with previous DSC results showing similar thermal history effects for phospholipid lamellar phases in EAN.[64]

Figure 4 shows an example of the MLV → ULV transition in the SANS patterns of DSPC in d_3-EAF at 298K and 338K, together with respective model fits.

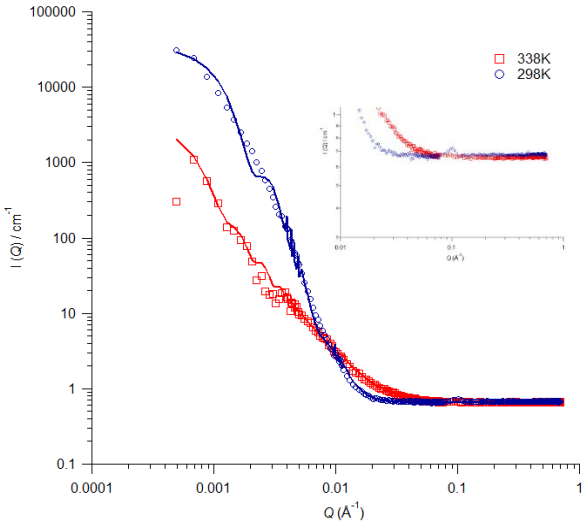

Figure 4. SANS data and fits for DSPC in d_3-EAF at 298K (MLV fit) and 338K (ULV fit), details of fitting parameters in Supplementary Information. Inset: zoomed image showing multi-lamellar peak.

The fitted bilayer thickness (Table 3) of unilamellar vesicles in ionic liquids suggest thicker bilayers, but also shows greater variation in best fit values. This is primarily due to difficulty in uniquely fitting the

solvated lipid polar groups, which is in part a consequence of the limited resolution at high *q* due to high incoherent scattering from partially deuterated ionic liquids. It is noteworthy, however, that the most water-like bilayer thicknesses are found in the least-nanostructured ILs, EtAF and DMEAF.

The repeat spacings between bilayers in MLVs (*D**) derived from the diffraction peak are also listed in Table 3 alongside fitted ULV bilayer thicknesses. These provide an independent measure of the upper bound of lipid bilayer thickness, including any solvent swelling, between adjacent bilayers. For DSPC in EAN the repeat spacing matches that found by Evans *et al*. [43]

*D** depends only weakly on temperature (relative to T_m). Where there was a measurable temperature dependence, a range is given. In all cases *D** is only slightly greater than the fitted thickness, and is smaller than the loose upper bounds obtained by fitting ULVs. This is consistent with there being little swelling and little solvent penetration between adjacent bilayers in MLVs.

Like egg PC, DMPC in PAN behaved differently to all other ILs. Its scattering pattern at all temperatures was best described by polydisperse but homogeneous spheres, consistent with microscopy results that showed no lamellar phase formation.

Table 3. Total lipid bilayer thickness of unilamellar vesicles from best fit to separated form factor model, together with bilayer repeat spacings of multilamellar vesicles.

	ULV Bilayer thickness and MLV repeat spacing (Å)			
	Egg PC	DMPC	DPPC	DSPC
D_2O	20- 40 (37-40)[62, 63]	35-45 (34-50)[17, 49, 52-55]	35-50 (36-50)[17, 48, 56, 57]	40-50 (49-52)[17, 65]
EAN	40-80	D* = 52	D* = 57	D* = 62-65
PAN	-	-	D* = 57-59	D* = 59
EAF	45-90 -	- D* = 54	- D* = 57-65	55-95 D* = 65
EtAF	46-70 -	- D* = 57	50-60 D* = 65	36-60 -
DMEAF	- -	- -	45-55 D* = 44	28-60 D* = 47

Discussion

Both isothermal penetration studies and dilute vesicle dispersions reveal that, while all the ILs examined support phospholipid self-assembly, many features depend strongly on the underlying nanostructure of the PIL. Phospholipids behave differently in amphiphilically nanostructured ILs (PAN, EAN and EAF) than they do in EtAF and DMEAF, which have little nanostructure.

Based on phospholipid behavior, EtAF and DMEAF are the most water-like of the ILs examined. This is surprising for DMEAF, as it lacks an H-bond network like water. This shows that the presence or ab-

sence of IL nanostructure is of greater consequence for phospholipid self-assembly than a hydrogen bond network.

Phospholipids most readily form ULVs with well-defined bilayers, and their chain melting enthalpies and entropies are very similar to aqueous systems. This suggests that the chain melting transition is relatively insensitive to head group solvation and ionic strength, whether in an IL or in aqueous solution. Some differences do emerge for shorter phospholipid acyl chains (DMPC), but these are consistent with expectations based on higher solubility and a weaker solvophobic driving force in these ILs than the hydrophobic effect in water.

The structures formed and phase transitions of these phospholipids in EAN are qualitatively different in PAN, which differs from EAN by a single methylene, and in EAF, which differs only in its counterion. PAN is thus less polar on average than EAN, which leads to higher solubilities of nonpolar moieties with nonspecific intermolecular interactions including alkanes and alkanols[10, 66] and also surfactant alkyl chains.[67, 68] However, by this measure it should also be less polar on average than DMEAF.[21, 67]

Previous work has shown that the extent and strength of the amphiphilic nanostructure in these ILs increases in the order EAF < EAN < PAN.[30] Nanostructure has two elements that affect phospholipid assembly. First is the strength of the coulombic and H-bond network of the polar domains, and second is the size of the solvophobically-segregated non-polar domains. Both have been shown to affect the solubility and association of aliphatic alkanols dissolved in these ILs.[66, 69]

PAN forms larger non-polar domains than either EAF or EAN, and these can accommodate longer alkyl chains, raising solubility and reducing the driving force towards the formation of micelles, microemulsions and lyotropic phases.[21, 67] This explains the lack of order seen in DMPC and egg PC dispersions in PAN.

Chain melting enthalpies are also uniformly lower in amphiphilic ILs because the cation alkyl chains can act as cosurfactants to stabilize the liquid-like acyl chains in the L_α phase. IL nanostructure reduces the energy cost associated with increasing the polar/nonpolar interfacial area that typically accompanies chain melting.

Both the optical microscopy (flooding) experiments and SANS patterns show that the nitrate ILs are less effective at swelling a lamellar phase and enabling lipid vesicle formation than are formate ILs, including EAF. For the phospholipids examined, all formate ILs readily produce a swellable lamellar phase, and can be used to prepare unilamellar vesicle dispersions above T_m.

This can be explained by noting that the bulk liquid nanostructure in EAF is similar to but less pronounced than in EAN.[26] We have recently shown that in PAN-octanol mixtures, the alkyl chains readily reorganize to accommodate non-polar alkyl chains, but that the network of polar domains comprised of H-bonded $–NH_3^+$ and NO_3^- ions remain intact, driving association of the alkyl groups.[69]

A similar situation arises in these phospholipids where the quaternary ammonium cannot H-bond, so the alkylammonium cation of the IL is responsible for H-bond solvation of the phosphate and carboxyl oxygens (see Figure 1). It should be more favourable to transfer an H-bond from a less-dense EAF network than from EAN or PAN. Thus the strength of the IL nanostructure provides a measure of the ease of lipid polar group solvation. It is therefore expected that different lipid polar groups will exhibit different sensitivities to cation and anion type.

IL nanostructure also influences the transition from MLV → ULV. Multilamellar to unilamellar vesicle transformation in these systems is clearly favoured by longer lipid alkyl chains, which indicates stronger segregation of the lipid bilayer from the solvent. For a given lipid, the MLV → ULV transition is favoured in less amphiphilic solvents, water, EtAF and (based on chain melting enthalpies) DMEAF. The formation of unilamellar vesicles in EAF by DSPC also fits this pattern.

The results obtained are generally consistent with previous studies of equilibrium phase behavior of DPPC, DMPC and DSPC, as well as other phospholipids in EAN.[27, 43, 64, 70] Tamura-Lis *et al*. report a (history-dependent) lamellar to hexagonal phase transition for 20 wt% DPPC in EAN at 329 K, slightly higher than our swelling or chain-melting temperatures, and an amorphous high-temperature structure for 20 wt% DMPC in EAN.[64] O'Leary and Levin have proposed that DPPC forms a micellar phase at 50 wt% in EAN at high temperatures based on Raman spectra showing disordered alkyl chains.[27] These results are consistent with our SAXS studies showing the presence of amorphous structures at high temperatures in both of these systems.

Conclusions

Phospholipids readily form bilayer-based assemblies in a range of protic ILs. As in water, increasing acyl chain length increases chain melting temperature and bilayer thickness, which are both almost insensitive to solvent.

However, the enthalpies of chain melting, as well as the swelling of lamellar phases and stability of ULVs compared with MLVs (or amorphous aggregates) depends strongly on the extent of underlying amphiphilic nanostructure in the ILs. This can be controlled by choice of cationic and anionic components of the ionic liquid. This conclusion can also be extended to understand lipid self-assembly in other exotic environments; the deep eutectic solvent choline chloride-urea does not exhibit amphiphilic nanostructure,[71] and it too supports vesicle self-assembly by phospholipids.[72]

Control over the formation of phospholipid ULVs and MLVs in ionic liquids presents new possibilities for nanoencapsulation and nanoreactors in these versatile solvents, while their stability suggests the use of protic ILs in biopreservation. The prospect of stable phospholipid membranes also provokes questions about the range of extreme environments in which life could potentially arise.[73]

Acknowledgements

We acknowledge funding from the Australian Research Council, and the support of the Bragg Institute, Australian Nuclear Science and Technology Organization, in providing the neutron research facilities used in this work. SJB thanks Australian Institute of Nuclear Science and Engineering for a post-graduate research award. Thanks to Dr Paul FitzGerald for assistance with the SANS experiments and for valuable discussions.

References

1. J. Hao and T. Zemb, *Curr. Opin. Colloid Interface Sci.*, 2007, **12**, 129-137.
2. T. L. Greaves and C. J. Drummond, *Chem. Rev.*, 2015, **115**, 11379-11448.
3. D. F. Evans, A. Yamauchi, R. Roman and E. Z. Casassa, *J. Colloid Interface Sci.*, 1982, **88**, 89-96.
4. M. U. Araos and G. G. Warr, *J. Phys. Chem. B*, 2005, **109**, 14275-14277.
5. R. Atkin and G. G. Warr, *J. Phys. Chem. B*, 2007, **111**, 9309-9316.
6. C. A. Angell, N. Byrne and J.-P. Belieres, *Acc. Chem. Res.*, 2007, **40**, 1228-1236.
7. M. Naushad, Z. A. Alothman, A. B. Khan and M. Ali, *Int. J. Biol. Macromol.*, 2012, **51**, 555-560.
8. F. Gayet, J.-D. Marty, A. Brûlet and N. L.-d. Viguerie, *Langmuir*, 2011, **27**, 9706-9710.
9. S. A. Forsyth, J. M. Pringle and D. R. MacFarlane, *Aust. J. Chem.*, 2004, **57**, 113-119.
10. T. L. Greaves and C. J. Drummond, *Chem. Soc. Rev.*, 2013, **42**, 1096-1120.
11. D. F. Evans, S.-H. Chen, G. W. Schriver and E. M. Arnett, *J. Am. Chem. Soc.*, 1981, **103**, 481-482.
12. C. Tanford, *Science*, 1978, **200**, 1012-1018.
13. T. J. McIntosh, A. D. Magid and S. A. Simon, *Biochemistry*, 1989, **28**, 7904-7912.
14. D. J. Hanahan, *A Guide to Phospholipid Chemistry*, Oxford University Press, USA, 1997.
15. R. Koynova and M. Caffrey, *Biochim. Biophys. Acta, Rev. Biomembr.*, 1998, **1376**, 91-145.
16. P. Stano and P. L. Luisi, *Chem. Commun.*, 2010, **46**, 3639-3653.
17. A. C. Woodka, P. D. Butler, L. Porcar, B. Farago and M. Nagao, *Phys. Rev. Lett.*, 2012, **109**, 058102.
18. B. J. Ravoo, W. D. Weringa and J. B. F. N. Engberts, *Langmuir*, 1996, **12**, 5773-5780.
19. B. A. Cornell, G. C. Fletcher, J. Middlehurst and F. Separovic, *Biochim. Biophys. Acta, Biomembr.*, 1982, **690**, 15-19.
20. P. Walde, *Orig Life Evol Biosph*, 2006, **36**, 109-150.
21. A. Dolan, R. Atkin and G. G. Warr, *Chem. Sci.*, 2015, **6**, 6189-6198.
22. L. J. Magid, Z. Han, G. G. Warr, M. A. Cassidy, P. D. Butler and W. A. Hamilton, *J. Phys. Chem. B*, 1997, **101**, 7919-7927.

23. C. R. López-Barrón, D. Li, L. DeRita, M. G. Basavaraj and N. J. Wagner, *J. Am. Chem. Soc.*, 2012, **134**, 20728-20732.
24. B. Fernández-Castro, T. Méndez-Morales, J. Carrete, E. Fazer, O. Cabeza, J. R. Rodríguez, M. Turmine and L. M. Varela, *J. Phys. Chem. B*, 2011, **115**, 8145-8154.
25. D. F. Evans, A. Yamauchi, G. J. Wei and V. A. Bloomfield, *J. Phys. Chem.*, 1983, **87**, 3537-3541.
26. R. Hayes, G. G. Warr and R. Atkin, *Chem. Rev.*, 2015, **115**, 6357-6426.
27. T. J. C. Leary and I. W. Levin, *J. Phys. Chem.*, 1984, **88**, 4074-4078.
28. R. Hayes, S. Imberti, G. G. Warr and R. Atkin, *Phys. Chem. Chem. Phys.*, 2011, **13**, 13544-13551.
29. R. Hayes, S. Imberti, G. G. Warr and R. Atkin, *Ang. Chem. Intl Ed.*, 2013, **52**, 4623-4627.
30. R. Hayes, S. Imberti, G. G. Warr and R. Atkin, *J. Phys. Chem. C*, 2014, **118**, 13998-14008.
31. D. Wakeham, R. Hayes, G. G. Warr and R. Atkin, *J. Phys. Chem. B*, 2009, **113**, 5961-5966.
32. A. Elbourne, K. Voitchovsky, G. G. Warr and R. Atkin, *Chem. Sci.*, 2015, **6**, 527-536.
33. R. G. Laughlin, *Adv. Colloid Interface Sci.*, 1992, **41**, 57-79.
34. Y. Maitani, in *Liposomes*, ed. V. Weissig, Humana Press, 2010, vol. 605, ch. 27, pp. 393-403.
35. R. Carlton, in *Pharmaceutical Microscopy*, Springer New York, 2011, DOI: 10.1007/978-1-4419-8831-7_2, ch. 2, pp. 7-64.
36. E. P. Gilbert, J. C. Schulz and T. J. Noakes, *Physica B: Condensed Matter*, 2006, **385–386, Part 2**, 1180-1182.
37. S. R. Kline, *J. Appl. Cryst.*, 2006, **39**, 895-900.
38. R. G. Laughlin, *The Aqueous Phase Behaviour of Surfactants*, Academic Press, San Diego, CA 92101, 1994.
39. L. S. Hirst, in *Fundamentals of Soft Matter Science*, Taylor and Francis, Boca Raton, FL, 2013, pp. 52-55.
40. F. B. Rosevear, *J. Amer. Oil Chem. Soc.*, 1954, **31**, 628-639.
41. W. J. Benton, in *Physics of Amphiphilic Layers*, eds. J. Meunier, D. Langevin and N. Boccara, Springer Berlin Heidelberg, 1987, vol. 21, ch. 28, pp. 207-209.
42. B. P. Gaber and J. P. Sheridan, *Biochim. Biophys. Acta, Biomembr.*, 1982, **685**, 87-93.
43. D. F. Evans, E. W. Kaler and W. J. Benton, *J. Phys. Chem.*, 1983, **87**, 533-535.
44. T. F. Gordon Aylward, *SI Chemical Data*, Jacaranda Wiley, Milton, QLD, Australia, 3 edn., 1994.
45. T. L. Greaves and C. J. Drummond, *Chem. Rev.*, 2008, **108**, 206-237.
46. G. F. A. Guinier, *Small-Angle Scattering of X-Rays*, John Wiley and Sons, New York, 1955.
47. B. Cabane, in *Surfactant Solutions: New Methods of Investigation*, ed. M. D. R. Zana, New York and Basel, New York, 1987, vol. 22.
48. M. A. Kiselev, P. Lesieur, A. M. Kisselev, D. Lombardo and V. L. Aksenov, *Appl Phys A*, 2002, **74**, s1654-s1656.
49. M. A. Kiselev, P. Lesieur, A. M. Kisselev, D. Lombardo, M. Killany and S. Lesieur, *J. Alloys and Compounds*, 2001, **328**, 71-76.
50. M. A. Kiselev, P. Lesieur, A. M. Kisselev, C. Grabielle-Madelmond and M. Ollivon, *J. Alloys and Compounds*, 1999, **286**, 195-202.
51. M. A. Kiselev, E. V. Zemlyanaya, V. K. Aswal and R. H. H. Neubert, *Eur Biophys J*, 2006, **35**, 477-493.
52. M. A. Kiselev, E. V. Zemlyanaya, N. Y. Ryabova, T. Hauss, S. Dante and D. Lombardo, *Chem. Phys.*, 2008, **345**, 185-190.

53. E. V. Zemlyanaya, M. A. Kiselev, J. Zbytovska, L. Almasy, V. K. Aswal, P. Strunz, S. Wartewig and R. Neubert, *Crystallogr. Rep.*, 2006, **51**, S22-S26.
54. J. Preu, T. Jaeger, V. Garamus and T. Gutberlet, *Eur Biophys J*, 2011, **40**, 687-698.
55. M. B. Boggara and R. Krishnamoorti, *Langmuir*, 2009, **26**, 5734-5745.
56. H. J. Risselada and S. J. Marrink, *Phys. Chem. Chem. Phys.*, 2009, **11**, 2056-2067.
57. P. C. Mason, B. D. Gaulin, R. M. Epand, G. D. Wignall and J. S. Lin, *Phys. Rev. E*, 1999, **59**, 3361-3367.
58. N. Kučerka, M. Kiselev and P. Balgavý, *Eur Biophys J*, 2004, **33**, 328-334.
59. T. Nawroth, H. Conrad and K. Dose, *Physica B: Condensed Matter*, 1989, **156–157**, 477-480.
60. V. I. Gordeliy, V. G. Cherezov and J. Teixeira, *Journal of Molecular Structure*, 1996, **383**, 117-124.
61. J. F. Nagle and S. Tristram-Nagle, *Biochim. Biophys. Acta, Rev. Biomembr.*, 2000, **1469**, 159-195.
62. S. Komura, Y. Toyoshima and T. Takeda, *Japanese Journal of Applied Physics*, 1982, **21**, 1370.
63. J. T. Mason and C. Huang, *Annals of the New York Academy of Sciences*, 1978, **308**, 29-48.
64. W. Tamura-Lis, L. J. Lis and P. J. Quinn, *J. Colloid Interface Sci.*, 1992, **150**, 200-207.
65. P. Balgavý, M. Dubničková, N. Kučerka, M. A. Kiselev, S. P. Yaradaikin and D. Uhríková, *Biochim. Biophys. Acta, Biomembr.*, 2001, **1512**, 40-52.
66. H. J. Jiang, P. A. FitzGerald, A. Dolan, R. Atkin and G. G. Warr, *J. Phys. Chem. B*, 2014, **118**, 9983-9990.
67. R. Atkin, S. M. C. Bobillier and G. G. Warr, *J. Phys. Chem. B*, 2009, **114**, 1350-1360.
68. I. L. Topolnicki, P. A. FitzGerald, R. Atkin and G. G. Warr, *ChemPhysChem*, 2014, **15**, 2485-2489.
69. T. Murphy, R. Hayes, S. Imberti, G. G. Warr and R. Atkin, *Physical Chemistry Chemical Physics*, 2016, **18**, 12797-12809.
70. W. Tamura-Lis, L. J. Lis and P. J. Quinn, *The Journal of Physical Chemistry*, 1987, **91**, 4625-4627.
71. O. S. Hammond, D. T. Bowron and K. J. Edler, *Green Chemistry*, 2016, **18**, 2736-2744.
72. S. J. Bryant, R. Atkin and G. G. Warr, *Soft Matter*, 2016, **12**, 1645-1648.
73. L. Ojha, M. B. Wilhelm, S. L. Murchie, A. S. McEwen, J. J. Wray, J. Hanley, M. Masse and M. Chojnacki, *Nature Geosci*, 2015, **8**, 829-832.